



**Impact of Stereochemistry on Rheology and Nanostructure
of PLA-PEO-PLA Triblocks: Stiff Gels at Intermediate L/D-
lactide Ratios**

Journal:	<i>Soft Matter</i>
Manuscript ID	SM-ART-07-2018-001559.R1
Article Type:	Paper
Date Submitted by the Author:	10-Aug-2018
Complete List of Authors:	Yin, Xuechen; Stony Brook University, Department of Chemistry Hewitt, David; Stony Brook University, Department of Chemistry Quah, Suan; Stony Brook University, Department of Chemistry Zheng, Bingqian; Stony Brook University, Department of Chemistry Mattei, Gerard; Stony Brook University, Department of Chemistry Khalifah, Peter; Stony Brook University, Chemistry; Brookhaven National Laboratory, Chemistry Department Grubbs, Robert B.; Stony Brook University, Chemistry; Brookhaven National Laboratory, Center for Functional Nanomaterials Bhatia, Surita; Stony Brook University, Department of Chemistry



Journal Name

ARTICLE

Impact of Stereochemistry on Rheology and Nanostructure of PLA-PEO-PLA Triblocks: Stiff Gels at Intermediate L/D-lactide Ratios

Received 00th January 20xx,
Accepted 00th January 20xx

DOI: 10.1039/x0xx00000x

www.rsc.org/

Xuechen Yin,^a David R.O. Hewitt,^a Suan P. Quah,^a Bingqian Zheng,^a Gerard S. Mattei,^a Peter G. Khalifah,^{a,b} Robert B. Grubbs,^a and Surita R. Bhatia*^a

We report rheology and structural studies of poly(lactide)-poly(ethylene oxide)-poly(lactide) (PLA-PEO-PLA) triblock copolymer gels with various ratios of L-lactide and D-lactide in the PLA blocks. These materials form associative micellar gels in water, and previous work has shown that stereoregular triblocks with a L/D ratio of 100/0 form much stiffer gels than triblocks with a 50/50 L/D ratio. Our systems display an unexpected maximum in the storage modulus, G' , of the hydrogels at intermediate L/D ratio. The impact of stereochemistry on the rheology is very striking; gels with an L/D ratio of 85/15 have storage moduli that are ~1-2 orders of magnitude higher than hydrogels with L/D ratios of 100/0. No stereocomplexation is observed in the gels, although PLLA crystals are found for gels with L/D ratios of 95/5 and 90/10, and SANS results show a decrease in the intermicellar spacing for intermediate L/D ratios. We expect the dominant contribution to the elasticity of the gels to be intermicellar bridging chains and attribute the rheology to a competition between an increase in the time for PLA endblocks to pull out of micelles as the L/D ratio is increased and PLLA crystallization occurs, and a decrease in the number of bridging chains for micelles with crystalline PLA domains, as formation of bridges may be hindered by crowded crystalline PLA domains. These results provide a new strategy for controlling the rheology of PLA-based hydrogels for potential applications in biomaterials, as well as fundamental insights into how intermicellar interactions can be tuned via stereochemistry.

Introduction

Block copolymer gels have been extensively studied for a broad range of biomedical applications. Inspiration from biological polymers and gels, such as cellulose and spider silk, which often contain well-organized or crystalline domains within a softer matrix, has led researchers to explore similar types of strategies with block copolymers where one of the blocks can form structures such as crystallites, helices, or beta sheets. This strategy has most often been employed in synthetic block polypeptides and block copolymers containing PEO and poly(lactic acid) (PLA). Among various polymeric materials, copolymers of PLA and PEO have received considerable attention due to the general biocompatibility of both PEO and PLA, and the biodegradability of PLA¹⁻¹⁰. Derived from renewable natural resources (e.g., sugar or corn)¹¹, PLA can also be considered to be a sustainable polymeric material¹², and as such it is desirable to explore new strategies

to tune the range of properties that can be achieved with PLA-based materials.

Several studies on aqueous solutions and hydrogels formed from diblock and triblock copolymers containing PLA and PEO have explored the dependence of the self-assembly and rheological properties on block length, sequence of blocks, and polymer concentration¹³⁻¹⁶. PLA-PEO-PLA triblock copolymers have been shown to form micellar structures in water and have been found to undergo a sol-gel transition as polymer concentration is increased, with the sol-gel transition depending upon block length^{9,17}.

One strategy to tune the properties of these materials is by blending systems containing both poly(L-lactic acid), or PLLA, and poly(D-lactic acid), or PDLA, to form a stereocomplex, sometimes referred to as sc-PLA. The presence of crystalline domains comprising these stereocomplexes is known to strongly influence the thermal and mechanical properties of the resulting gels and solids. The use of stereocomplexation of PLA to form hydrogels of P(HEMA)-graft-oligo(LA) was first reported in 2000¹⁸. More recent studies have focused on gels of block copolymers containing both PLLA and PDLA blocks, as reviewed recently¹⁹. Fujiwara and Kimura demonstrated that temperature-dependent, injectable hydrogels could be formed by inducing stereocomplex formation of enantiomeric micelle mixtures of PLA-PEO-PLA triblock copolymer²⁰. The presence

^a Department of Chemistry, Stony Brook University, Stony Brook, NY 11794, USA.

^b Department of Chemistry, Brookhaven National Laboratory, Upton, NY 11793, USA.

*Corresponding author: Surita.bhatia@stonybrook.edu

Electronic Supplementary Information (ESI) available: Representative NMR spectra, additional rheological data. See DOI: 10.1039/x0xx00000x

of these stereocomplexes led to formation of very strong junction points within the physically associated hydrogel, and the resulting materials were explored for drug release, bioimaging, and tissue engineering scaffolds¹⁹.

The stereoregularity and monomer sequence of PLA-based block copolymers is also known to impact their microstructure and mechanical properties. The polymerization of lactic acid can generate isotactic, syndiotactic, atactic and heterotactic PLA blocks comprising PLLA, PDLA, or blocks with mixtures of the L- and D-lactide units. Meyer and coworkers have applied segment assembly polymerization (SAP) to the synthesis of copolymers of lactic acid and glycolic acid to obtain polymers with well-controlled monomer sequences²¹⁻²³. They found that specific sequences of monomers within their poly(lactic-co-glycolic acid) (PLGA) materials displayed diminished swelling and slower erosion behavior compared to random PLGA copolymers, indicating the dramatic dependence of degradation behavior on the monomer sequence²³.

Another strategy to achieve crystalline domains within hydrogels is through the use of copolymers with stereoregular blocks. Tew and Bhatia have previously reported the creation of associative PLA-PEO-PLA hydrogels with crystalline PLA domains, PLLA-PEO-PLLA; and have compared the assembly, rheology, and release characteristics of these gels with gels formed from copolymers synthesized with a racemic mixture of L-lactide and D-lactide, e.g. an L/D-lactide ratio of 50/50. Wide-angle X-ray diffraction (WAXD) data²⁴ on systems with L/D ratios of 100/0 show peaks that are characteristic of crystalline PLLA²⁵, and samples with L/D ratios of 50/50 show no evidence of PLA crystals. The crystallites present in the PLLA-PEO-PLLA systems persist even when the polymers are hydrated in the gel state. SANS experiments²⁶ yielded spectra that fit well to models of spherical micelles for systems with a L/D ratio of 50/50, and flat disk-shaped micelles for polymers with an L/D ratio of 100/0. This is consistent with the concept that the stereoregular polymers form crystalline domains. The difference in the nanoscale structure has important implications for the rheology of these systems. For the PLLA-PEO-PLLA systems with crystalline domains, the storage modulus, G' , is found to depend strongly on the length of the PLA block for triblocks with the total number of PLA repeat units (RU_{PLA}) when RU_{PLA} is less than about 70; the dependence becomes much weaker for longer PLA blocks^{24, 27}. Moreover, in comparing the rheology of gels with the same polymer molecular weight and concentration, it is found that the presence of crystalline PLA domains results in an increase in G' of up to three orders of magnitude at low frequencies²⁴.

Here, we report on the effect of varying the L/D ratios of PLA blocks on the structure and rheology of hydrogels containing PLA-PEO-PLA copolymers. Small-angle neutron scattering (SANS) was used to quantify the self-assembly of these polymers and the nanostructure of the resulting gels, and small amplitude oscillatory shear rheology was used to characterize the mechanical and flow properties of the gels. As discussed further below, the percentage of D-lactide and L-lactide in PLA structure are seen to have a significant and nonmonotonic effect on the elastic modulus of gels, and this

appears to be correlated with stronger interactions between micelles observed through SANS. These studies provide insight into the impact of stereochemistry on the structure and rheology of these systems and widen the envelope of mechanical properties that can be achieved with PLA-based associative hydrogels.

Experimental

Materials and triblock copolymer synthesis

L-Lactide and a racemic mixture of D-lactide and L-lactide from Acros Organics and Sigma Aldrich were both recrystallized from either ethyl acetate or toluene and stored in the glove box. Polyethylene oxide (PEO-10k, $M_n = 10$ kg/mol, Alfa Aesar) was freeze-dried or vacuum dried at 40 °C for two days before storing in the glove box prior to polymerizations²⁸. 1,8-Diazabicyclo[5.4.0]undec-7-ene (DBU) was obtained from Santa Cruz Biotechnology. All required solutions were prepared in nanopure water with resistivity set at 18MΩ-cm.

The detailed synthesis method is based on previously reported approaches^{17, 29-31}. PEO-10k (1.2 g, 0.12 mmol) in a round-bottom flask equipped with a magnetic stir bar was sealed with a rubber septum and removed from the glove box. Re-crystallized D,L-lactide (0.62 g, 4.3 mmol) was removed from the glove box in a scintillation vial and dichloromethane (12 mL) was added via a nitrogen-purged syringe. The vial was swirled to ensure complete dissolution with the syringe still inserted. Using the same syringe, the lactide solution was subsequently added to the round-bottom flask containing the PEO-10k. A solution of DBU (0.04 g, 0.26 mmol) in dichloromethane (4.0 mL) was prepared in the glove box, and transferred by syringe to the round-bottom flask containing the PEO-10k/lactide solution. The reaction was allowed to proceed for 4 hrs at room temperature. After 4 hrs the polymerization mixture was concentrated by a rotary evaporator. The crude polymer was then precipitated by addition into hexanes (70 mL). The supernatant was subsequently decanted, and the solid polymer was dried in a vacuum oven at 40 °C for 3 days. Typical yields were >80%, with monomer conversions >95% determined by ¹H NMR (400 MHz, CDCl₃), by comparison of polymer methine protons to residual monomer methine protons. ¹H NMR of isolated PLA-PEO-PLA (400 MHz, CDCl₃): δ 5.17 (m, -OOC-CH(CH₃)-), 4.32 (m, -OOC-CH(CH₃)-OH), 4.21 (m, COO-CH₂-CH₂-OPEO), 3.56 (m, -CH₂-CH₂-O-), 1.57 (d, -OOC-CH(CH₃)-). (Supporting information).

Preparation of polymer solutions and gels

Each gel was prepared by the slow addition of a dried PLA-PEO-PLA sample, over about two hours, to a fixed volume of nanopure water followed by stirring with a magnetic stir bar. When the viscosity of solution increased to the point where magnetic stirring was no longer effective, manual stirring with spatula was employed until the polymer was completely added and the mixtures appeared homogeneous. The solutions were allowed to equilibrate for at least one day at room

temperature in sealed vials to ensure full dissolution of polymers in the nanopure water. For each polymer investigated, samples were made at concentrations of 10%, 12%, 15%, 18%, and 20% by weight. For gel samples used for SANS, the preparation procedure was similar, except that D₂O was used as the solvent.

Rheological characterization

Small amplitude oscillatory shear studies were performed using a TA Instruments stress-controlled AR-G2 rheometer. The gels were transferred onto the Peltier plate and were trimmed to fit a parallel plate (40 mm) or cone-and-plate (40 mm, 2° cone) geometry which were used to perform the stress sweeps and frequency sweeps. The gels and geometry were covered by a solvent trap to avoid evaporation of water. Amplitude sweeps were performed before the frequency sweeps to ensure that all experiments were performed within the linear viscoelastic regime. All tests were performed at 25°C.

SANS characterization

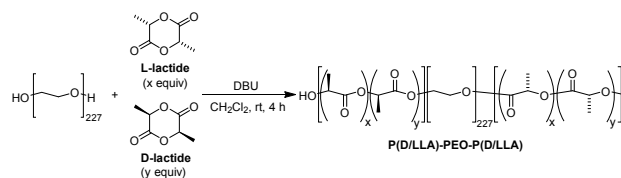
SANS measurements were conducted on the Extended Q-range Small-angle Neutron Scattering diffractometer (beamline 6, EQ-SANS) at the Spallation Neutron Source (SNS) located at Oak Ridge National Laboratory (ORNL), Oak Ridge, TN. Spectra were obtained at 25°C for all the samples. The q range covered in experiments was $0.002 \text{ \AA}^{-1} < q < 0.1 \text{ \AA}^{-1}$. The low-angle detector can travel along the beam, giving a variable sample to detector distances of 1.3 to 9 m. Data reduction and normalization were performed using standard techniques, and all SANS data reported here are on an absolute scale except where noted.

XRD and WAXS characterization

Wide-angle X-ray scattering (WAXS) was performed on gels at 10 wt% polymer concentration at the CMS (11-BM) beamline at the National Synchrotron Light Source II (NSLS-II), Brookhaven National Laboratory (BNL). The energy of the beam was 13.5 keV, which corresponds to a wavelength of 0.9814 Å. The q range covered in experiments was $0.2 \text{ \AA}^{-1} < q < 4.2 \text{ \AA}^{-1}$. Gels were confined between two glass slides, sealed with Parafilm M (Sigma Adrich). Samples were measured at room temperature in air, and empty glass slides were used for background subtraction. Laboratory XRD WAXS experiments were carried out on a Bruker D8 Advance diffractometer (Cu K α source) in the Bragg-Brentano geometry with a 217.5 mm radius and a 192 channel Lynx-Eye detector. Powder samples were placed on a zero-background Si crystal disc, and data were collected over a 2θ range of 8 – 67° (corresponding to a q range of $0.569 \text{ \AA}^{-1} < q < 4.50 \text{ \AA}^{-1}$) with a step size of 0.04° and a count time of 1s/step/channel. No corrections were made for sample height or sample transparency effects.

Results and discussion

Triblock copolymer synthesis



Scheme 1 Synthesis of triblock copolymers with varying L/D ratio.

A series of PLA-PEO-PLA triblock polymers were synthesized by DBU-catalyzed polymerization of solutions comprising a racemic mixture of D-lactide and L-lactide, with added L-lactide in amounts to provide the desired L/D ratio in the final polymers, from the terminal hydroxyl groups of poly(ethylene oxide) (PEO, $M_n = 10.0 \text{ kg/mol}$) for rheological study and SANS (Scheme 1). The length of PEO block and target length of PLA block were kept constant while the percent of PLLA and PDLA in PLA block were varied (Table 1). Previous studies with the similar but more basic organocatalyst 1,5,7-triazabicyclo[4.4.0]dec-5-ene (TBD) show minimal epimerization during polymerization of *rac*-lactide, and a only a slight isotactic enhancement for adding to a D-lactide chain end.³² DBU has been used to prepare linear PLLA,³³ PDLA/PLLA stars,³⁴ and other architectures with no racemization reported. Based on these literature studies, we do not expect a significant reactivity difference between L-lactide and D-lactide, and we expect our final polymers to have L/D ratios equal to the feed, with a nearly statistical distribution of L-L and D-D dimeric units. Previous DSC studies of PLA block copolymers³⁵ have shown that polymers with L/D ratios below 80/20 do not exhibit crystallinity and are essentially amorphous; thus, we targeted L/D ratios between 75/25 and 95/5, rather than cover the entire range between 50/50 and 100/0.

As can be seen in Table 1, there is a slight variation in the PLA block lengths in each series of polymers. However, the variation within each series of polymers is small, and we do not expect this to significantly impact the rheological behavior and nanostructure. For example, although the storage modulus of PLLA-PEO-PLLA hydrogels was found to depend strongly on PLA block length for systems where $RU_{PLA} (2x + 2y)$ in Scheme 1) was varied from 52 to 74²⁷, almost no increase was observed in the storage modulus for samples where RU_{PLA} was varied in the range 72 – 82.²⁴ SANS spectra for solutions and gels of PLA-PEO-PLA copolymers with constant PEO block lengths also showed very little variation for $RU_{PLA} = 77 – 87$ ²⁶. The range of RU_{PLA} for our rheology studies (series 1) was 70 – 77, and for our SANS studies (series 2) was 75 – 88. Again, while the differences in molecular weight are small within each series, we do discuss possible impacts on the observed rheology and nanostructure below.

Table 1. Characteristics of PLA-PEO-PLA triblock copolymers synthesized

Sample, rheology series	\bar{D}^a	Total RU _{PLA} (obs.) ^b	L/D ratio	Sample, SANS series	\bar{D}	Total RU _{PLA} (obs.)	L/D ratio
S ₁ 50/50	1.27	74	50/50	S ₂ 50/50	1.21	88	50/50
S ₁ 75/25	1.06	74	75/25	S ₂ 75/25	1.16	75	75/25
--	--	--	--	S ₂ 80/20	1.21	82	80/20
S ₁ 85/15	1.06	72	85/15	S ₂ 85/15	1.10	77	85/15
S ₁ 90/10	1.09	77	90/10	S ₂ 90/10	1.22	81	90/10
S ₁ 95/5	1.07	74	95/5	S ₂ 95/5	1.17	85	95/5
S ₁ 100/0	1.25	70	100/0	S ₂ 100/0	1.26	82	100/0

^a Dispersity, \bar{D} , determined by size-exclusion chromatography in THF with polystyrene standards. ^bTotal lactide repeating units (RU_{PLA}) and L/D ratio determined by ¹H NMR spectroscopy.

Rheological studies

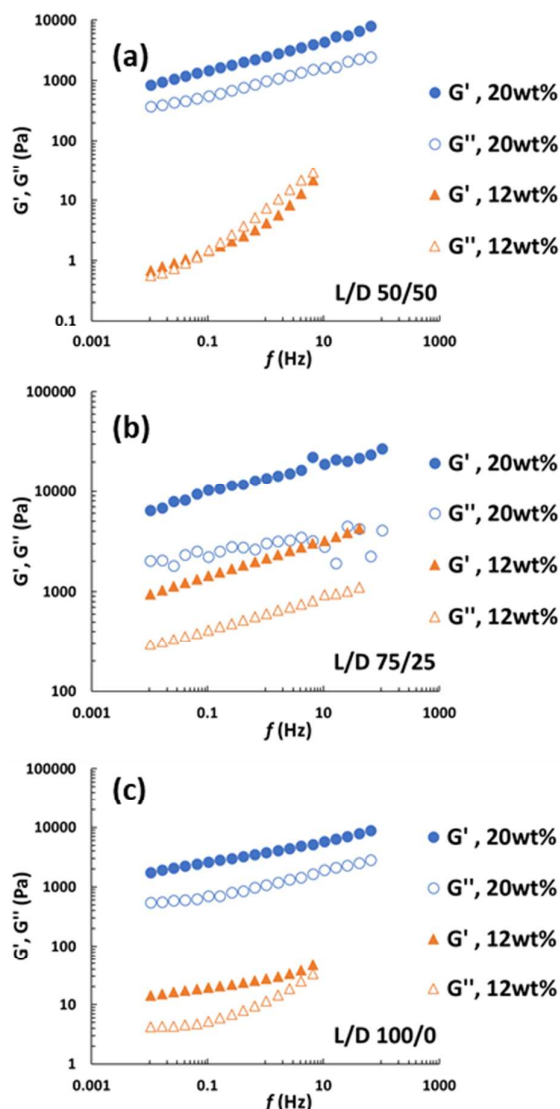


Figure 1. Representative frequency sweeps of PLA-PEO-PLA triblock copolymer gels with varying L/D ratio, (a) S₁ 50/50, (b) S₁ 75/25, and (c) S₁ 100/0, at different concentrations.

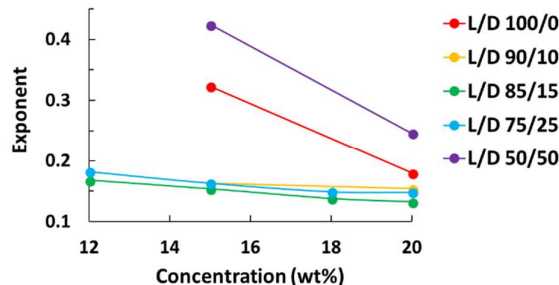


Figure 2. Exponents for samples displaying critical behaviour as a function of concentration and L/D ratio.

Figure 1 shows the storage moduli, G' , and loss moduli, G'' , of representative systems at polymer concentrations of 20 wt% and 12 wt% in water. Data on all polymers and at additional concentrations can be found in the Supporting Information (Figure S4–S5). For all polymers, samples at 20 wt% displayed gel-like behavior, with G' greater than G'' over the measurable frequency range of 0.01 Hz – 10 Hz. In comparison to the 20 wt% samples, some polymers showed characteristics of viscoelastic liquids at lower concentrations. For example, at 12 wt%, S₁ 50/50 exhibited $G'' > G'$ between 0.1 – 10 Hz, and both viscoelastic moduli showed a strong frequency dependence, indicative of relaxation of the system.

For samples displaying critical behavior, we fit the moduli data to the form $G' \sim G'' \sim f^m$, and found exponents in the range of 0.13 – 0.42. These exponents are summarized in Figure 2. The value of this exponent is sometimes interpreted to be indicative of the topology of the polymer network present in the gel, although it can be affected by polymer-solvent interactions. Similar rheological analyses performed on physically associated biopolymer gels^{36, 37} and transient networks of triblock copolymers³⁸ have yielded exponents in the range 0.5–0.7, while gels containing semicrystalline domains, including gels of bacterially-derived poly(β -hydroxyoctanoate)³⁹ have yielded exponents as low as 0.11. The power law exponents we obtain are indicative of soft solid behavior⁴⁰, and in general, lower values indicate weaker dependence of the moduli on frequency and more solid-like character of the gels. For example, exponents of 0.25 and 0.18 were obtained for the S₁ 50/50 gel and S₁ 100/0 gel at 20 wt%, respectively. It is noteworthy that an even weaker frequency-dependence was observed for the S₁ 85/15 gel, with a power-law exponent 0.13. This may indicate a possibly stronger interaction between micelles for this system, leading to a stiffer, more solid-like network. The damping factor ($\tan \delta$) is consistent with this behavior, as described further in the Supplemental Information (Figures S6 and S7). A similar type of stiffening has been observed in stereocomplex-forming PLA-based gels¹⁹ and hydrogels formed from heterochiral mixtures of peptides;⁴¹ however, as discussed further below, diffraction data show no evidence of stereocomplexes in the gels, and this is consistent with previous studies on PLA homopolymers with similar L/D ratios.

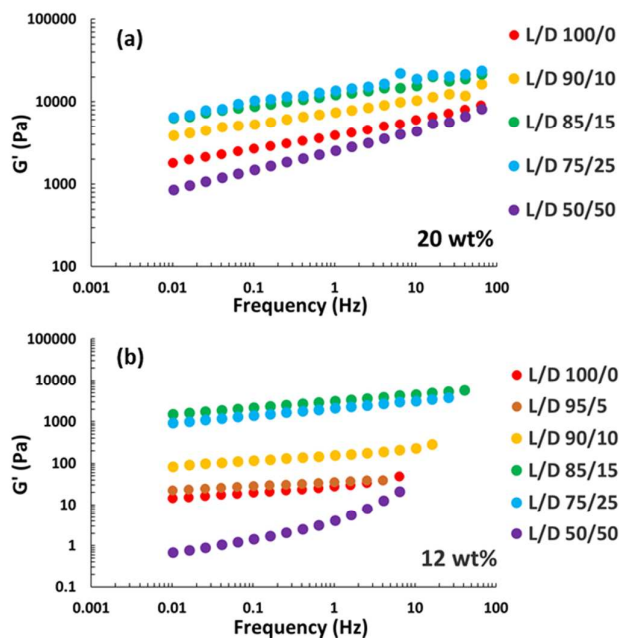


Figure 3. Effect of stereochemistry on the rheological properties. Frequency stress sweep of PLA-PEO-PLA triblock copolymer gels with different L/D ratios at (a) 20 wt% and (b) 12 wt%.

Interestingly, the critical exponents of the 100/0 and 50/50 gels increase at lower concentration, while the critical exponents of the 75/25, 85/15, and 90/10 gels are not strongly dependent upon concentration (Figure 2). This suggests that the network structure being formed by the polymers at intermediate L/D ratios is not being disrupted over the concentration range that we have explored. In principle, a Winter-Chambon analysis⁴² can also be performed to provide another measure of the gel strength and gain some insight into how the gel strength and network varies with stereochemistry; however, we had only a limited set of samples that displayed critical behavior.

The storage moduli G' of gel samples with different L/D ratios at two representative concentrations are displayed in Figure 3. Interestingly, varying the L/D ratio results in striking non-monotonic changes in the storage modulus. That is, gels with intermediate L/D ratios (S_1 75/25 and S_1 85/15) are stiffer and display a higher storage modulus than both the S_1 50/50 and the S_1 100/0 systems. Moreover, comparing the data at 20 wt% (Figure 3a) and 12 wt% (Figure 3b), it is apparent that this effect becomes more significant at lower polymer concentrations. Data at additional concentrations is provided in the Supplemental Information (Figure S5).

The higher G' for the S_1 75/25 and S_1 85/15 systems as compared to the S_1 50/50 system is perhaps not surprising; previous work comparing the rheology of PLA-PEO-PLA hydrogels with L/D ratios of 50/50 as compared to 100/0 has shown a significant increase in G' for the 100/0 systems due to

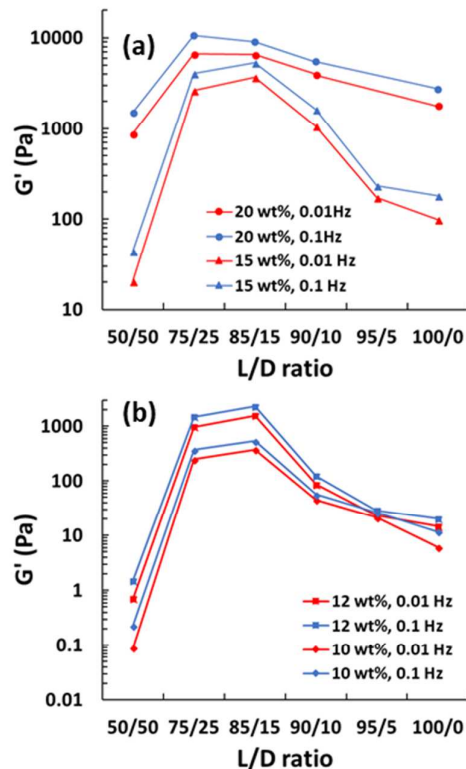
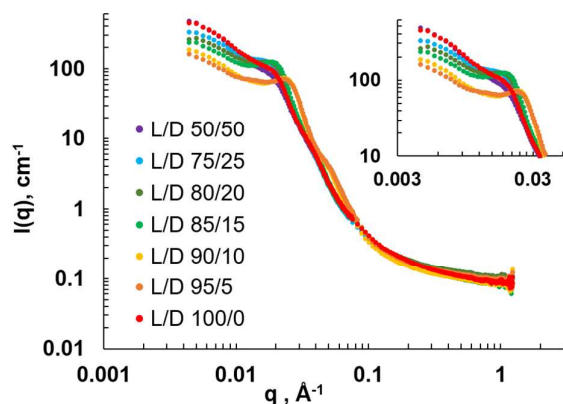


Figure 4. Variation of the storage modulus at 0.01 Hz and 0.1 Hz for gels at (a) 20 wt% and 15 wt% and (b) 12 wt% and 10 wt%.

the presence of crystalline domains in the stereoregular 100/0 system²⁴. However, we would expect that the PLA domains in hydrogels formed from polymers with intermediate L/D ratios to be semicrystalline in nature and perhaps to lead to weaker gels with a storage modulus that is in between than of the 50/50 and 100/0 systems. Instead, we find that the storage moduli for the S_1 75/25 and S_1 85/15 hydrogels to be approximately one order of magnitude greater than G' for the S_1 100/0 hydrogel at 20 wt%, and about two orders of magnitude greater at 12 wt%. This effect is summarized in Figure 4.

Additionally, although there is some small variation of PLA block length in this series (RU_{PLA} varies from 70–77), we do not expect that changes in the rheology of this magnitude will be strongly influenced by such a small change in the molecular weight. Indeed, as described above, previous studies of PLA-PEO-PLA hydrogels found a strong dependence of G' on PLA block length for RU_{PLA} between 52 to 74, but almost no increase in G' ²⁴ for samples where RU_{PLA} was varied between 72 and 82^{24,27}. The general trend we observe for the variation of G' with L/D ratio is 75/25 \approx 85/15 $>$ 90/10 $>$ 95/5 $>$ 100/0 $>$ 50/50.

SANS experiments



SANS was conducted on copolymers with varying L/D ratios

Figure 5. SANS spectra of copolymer gels with different L/D ratio at 10 wt% concentration in D₂O. Inset: Enlarged portion of the area around the correlation peak.

to study the effect of lactide block stereochemistry on micelle self-assembly and interaction. Lower concentrations (10wt%) were used for these studies to facilitate ease of sample loading. Generally speaking, small-angle scattering from micellar gels typically shows two features: a primary peak, which may be quite broad, which characterizes the intermicellar spacing and intermicellar interactions; and the decay of the intensity at higher wavevectors q , arising from the tail of the single-particle form factor. In between the peak and the high q range, oscillations from the micelle form factor may be observed; or higher order of peaks may exist, depending upon the degree of ordering of the micelles. The presence of any form factor oscillations and higher-order peaks may be smeared by polydispersity effects and instrumental resolution. With self-assembled micelles, there is typically some polydispersity present in the micelle size that dampens higher-order peaks and oscillations.

SANS spectra for a series of PLA-PEO-PLA gels at 10 wt% and varying L/D ratios are shown in Figure 5. A broad correlation peak is observed for all the gels in this series. No strong higher-order peaks are observed, suggesting that the micelles are disordered and do not arrange into any type of cubic structure, as is observed in some micellar gels. The peak position, q_{max} can be used to obtain an approximate distance between scattering centers within the gel, $d = 2\pi/q_{\text{max}}$. It is commonly understood that as concentration increases, the distance between micelles decreases, and hence the peak position increases or shifts to higher q . Interestingly, although these data are at the same polymer concentration, we clearly see a shift of the peak position to higher q for samples S₂ 85/15, S₂ 90/10, and S₂ 95/5 (Figure 5, inset). Table 2 shows the intermicellar distance derived from the peak position,

which shows a decrease in the micellar distance for samples with intermediate L/D ratios. The extent to which this change in the d -spacing is related to our rheological results is discussed further below. Our rheology also shows an increase in G' at intermediate L/D ratio, although the specific L/D ratio at which the minimum intermicellar distance occurs, 95/5, is different than that corresponding to the maximum observed in rheology, which is 85/15 for the gels at 12 wt%. Some of this discrepancy may be due to the variation in PLA block length between the series used for rheology ($RU_{\text{PLA}} = 70 - 77$) and SANS ($RU_{\text{PLA}} = 77 - 88$), or there may be an effect of polymer concentration, since the L/D ratio at which the maximum in G' occurs is higher for the 10-15 wt% gels as compared to the 20 wt% systems (Figure 4).

Table 2. Estimated d -spacing calculated from correlation peaks in SANS spectra.

Sample, SANS series	d -spacing (Å)
S ₂ 50/50	356
S ₂ 75/25	350
S ₂ 80/20	345
S ₂ 85/15	314
S ₂ 90/10	253
S ₂ 95/5	241
S ₂ 100/0	323

XRD and WAXS results

X-ray diffraction studies were used to gain insights into the type and degree of crystallinity in both dry solid powders (Figure 6) and in hydrated gels (Figure 7). Figure 6 shows laboratory XRD results on the S₂ 50/50 powder, S₂ 100/0 powder, and PEO powder (MW ~ 300,000 g/mol, Sigma Aldrich), while Figure 7 shows WAXS spectra on the S₂ 50/50, S₂ 75/25, S₂ 80/20, S₂ 90/10, and S₂ 95/5 gels at 10 wt% in water, with scattering from the glass sample holders subtracted. Intensities have been shifted vertically for clarity.

In the solid powder samples (Figure 6), a strong peak at $q = 1.36 - 1.37 \text{ \AA}^{-1}$ is observed both for the PEO homopolymer and for copolymers containing PEO, indicating the presence of crystalline PEO domains. This PEO peak has been previously reported as the (120) reflection of crystalline PEO (monoclinic, $a = 8.05 \text{ \AA}$, $b = 13.04 \text{ \AA}$, $c = 19.48 \text{ \AA}$, $\beta = 125.4^\circ$).^{43, 44} In PLLA-PEO copolymers, this PEO peak can overlap with the (203) and (113) reflections of crystalline PLLA domains (orthorhombic, $a = 10.6 \text{ \AA}$, $b = 6.1 \text{ \AA}$, $c = 28.8 \text{ \AA}$).⁴³⁻⁴⁶ All samples also show a series of overlapped PEO peaks centered around $q 1.66 \text{ \AA}^{-1}$, which have previously been assigned as the (032), ($\bar{1}$ 32), and ($\bar{2}$ 1 $\bar{2}$) reflections of this phase. The 100/0 sample additionally shows a peak at $q = 1.2 \text{ \AA}^{-1}$, which is attributed to the (110) and (200) reflections of PLLA based on literature precedent.^{25, 43, 45, 46}

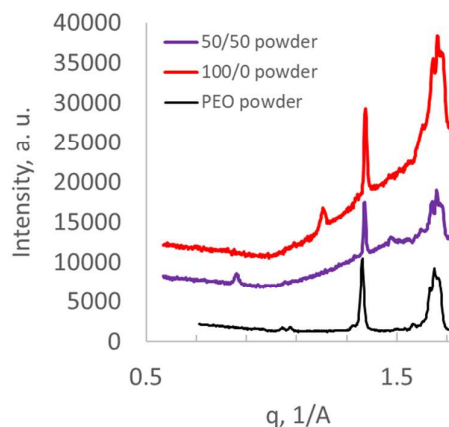


Figure 6. Lab XRD of solid powders of S_2 50/50 and S_2 100/0 polymers, compared to crystalline PEO. Intensities have been shifted in the vertical direction for clarity.

In contrast, the 50/50 solid powder does not show any evidence of PLLA crystallinity as evidenced by the lack of intensity at the peak positions discussed above. However, there is evidence for a small amount of stereocomplexation in this sample. PDLA-PLLA stereocomplexes (triclinic unit cell, $a = 9.16 \text{ \AA}$, $b = 9.16 \text{ \AA}$, $c = 8.70 \text{ \AA}$, $\alpha = 109.2^\circ$, $\beta = 109.2^\circ$, $\gamma = 109.8^\circ$)⁴⁵ typically show peaks at $q = 0.85 \text{ \AA}^{-1}$ and 1.49 \AA^{-1} . In the 50/50 solid sample, a small, broad peak at 0.85 \AA^{-1} is observed, and a very weak peak at $q = 1.49 \text{ \AA}^{-1}$ may be present, although it is difficult to discern. Thus, the presence of PLLA and PEO crystals in the 100/0 solid powder is evident, and the solid powder of the 50/50 sample also shows PEO crystals and perhaps a small amount of stereocomplexation. The presence of some stereocomplexes in the solid 50/50 sample is consistent with previous diffraction studies on solid and melt PLA homopolymers with varying L/D ratios, which show some evidence of stereocomplexation for L/D ratios between 40/60 and 60/40 (but not for samples outside of this range).⁴⁵

When the copolymers are in an aqueous solvent, it is expected that the PEO chains will become hydrated and the PEO regions will become amorphous. This is expected behavior is consistent with our WAXS data (Figure 7); the characteristic peaks of crystalline PEO (sharp peak at $q = 1.36 \text{ \AA}^{-1}$ and overlapping peaks at $q = 1.65\text{--}1.66 \text{ \AA}^{-1}$) are not observed in any of the gels. This is consistent with our previous studies of 100/0 and 50/50 gels.²⁴

Additionally, none of the gels show any evidence of stereocomplexation. There are no features at $q = 0.85 \text{ \AA}^{-1}$ or 1.49 \AA^{-1} . The very broad feature at lower q in the 75/25, 80/20, 85/15, and 90/10 samples is centered around $0.76\text{--}0.77 \text{ \AA}^{-1}$. PDLA/PLLA stereocomplexes are strong assemblies and typically persist even when polymers are hydrated and in the gel state. Although the 50/50 sample showed some indication of stereocomplex formation in the solid state, any complexes present seem to disassemble in the gel, suggesting that any structures that form in the solid state for our systems are fairly weak assemblies, perhaps because they are not comprised of sufficiently long runs of L- and D-lactide units. This is consistent

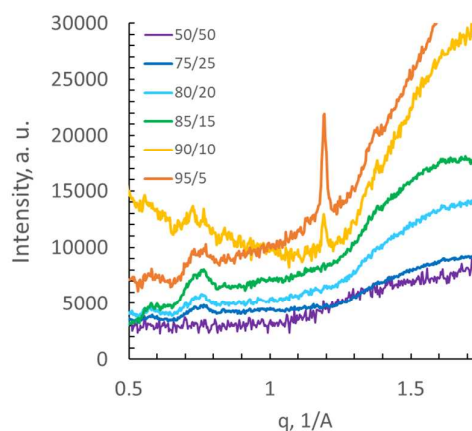


Figure 7. WAXS of the S_2 series gels at 10 wt% in water, with background from glass subtracted. Intensities have been shifted in the vertical direction for clarity.

with our expectation that the D-lactide units are distributed within the PLA blocks.

Our previous studies showed that PLLA crystallites are present in 100/0 triblocks even when the polymers were hydrated and in the gel state.²⁴ We observe similar behavior here for samples with a high content of L-lactide units, where gels with L/D ratios of 95/5 and 90/10 show evidence of PLA crystals via relatively sharp peaks at $q = 1.19 \text{ \AA}^{-1}$ (Figure 7). Additionally, although it is difficult to quantify given the weak scattering of these samples, the degree of crystallinity of the PLA domains does appear to systematically increase with increasing content of L-lactide units, which we would expect. Samples with lower L/D ratios do not show any evidence of PLLA crystallinity. However, it is possible that some PLLA crystallites that are either weakly ordered or too small to detect in WAXS are present in the 75/25, 80/20, and 85/15 samples, especially given the high background signal that arises from amorphous PEO and water. Even for the 90/10 sample, the PLLA peak is relatively small against the high background signal. Implications of this on the rheology are discussed further below.

Discussion of mechanism

In order to determine the mechanism behind the rheological behavior, we must discuss the various contributions to the elasticity in this system. Semenov et al.⁴⁷ and others have described the contributions of micellar deformation to the shear modulus of associative polymer gels, with the shear modulus increasing with effective volume fraction. In our system, it is possible that the self-assembly of the PLA-PEO-PLA triblocks varies with L/D ratio in such a way that there is a decrease in the micellar aggregation number at intermediate L/D ratios, followed by an increase for the S_2 100/0 polymer. It is, of course, very likely that both the shape and the aggregation number of micelles change with L/D ratio, and in general micelles with crystalline cores have higher aggregation numbers than those with amorphous cores due to the stronger driving force for assembly²⁶. It is not apparent what the thermodynamic driving force would be for the aggregation number to first decrease, and then increase, as

the L/D ratio is changed. However, if such an effect occurred, this would lead to an increase in the number density of micelles at intermediate L/D ratios. This is consistent with our SANS data, which show a decrease in the *d*-spacing at intermediate L/D ratios. However, the increase in the storage modulus is much stronger than what we would expect from our SANS studies. From SANS, the *d*-spacing at intermediate L/D ratios is 0.67-0.74 times that for the 50/50 and 100/0 samples. This corresponds to an increase in the volume fraction by a factor of 2.4-2.9. Based on the theory of Semenov and co-workers,⁴⁷ this would give rise to an increase in the storage modulus of 1.7-2.0 times, not the order-of-magnitude differences that we observe. Thus, it is unlikely that micellar crowding is the main contribution to the gel elasticity, and any changes in the effective volume fraction of micelles are not the cause of the rheological properties that we observe.

Another important contribution to elasticity in associative micellar gels is formation of intermicellar bridging chains, which build up a percolated network with a stress relaxation time that is exponentially related to the pull-out energy or strength of associative domains, χ_{as} .⁴⁸⁻⁵¹ Mattice and co-workers have reported simulations that demonstrate the strong effect χ_{as} has on the elasticity.⁵² However, another important consideration is the fraction of elastically effective chains, or fraction of chains that form bridges to the network. The storage modulus is also strongly dependent upon the fraction of bridging chains in associative gels.^{49, 50}

In our system, the associative strength is related to the energetics of the PLA micelle cores. If stereocomplexes were present at intermediate L/D ratios, we might expect that χ_{as} could vary with L-lactide content in a non-monotonic fashion, where the PLA domains are amorphous with low χ_{as} for the 50/50 gels, have strong stereocomplexes and very high χ_{as} for gels with lower L-lactide content (e.g., 75/25, 80/20, and 85/15) and include PLLA crystals with a χ_{as} that is lower than that of the stereocomplexes for gels with higher L-lactide content. Yet, WAXS does not show evidence of stereocomplexation in the gels, and the synthetic approach used should yield a nearly statistical distribution of L-L and D-D units in the PLA blocks, which would also not favor stereocomplexation. Instead, WAXS shows formation of PLLA crystals in the PLA domains for samples with high L/D ratios, and suggests that the degree of crystallinity, and hence χ_{as} , increases with L-lactide content.

However, we hypothesize that there is a competition between formation of PLLA crystals and the fraction of elastically effective bridging chains. Micelles may initially assemble in a state where intrachain PLA associations (leading to elastically ineffective PEO loops) are favored over interchain PLA associations (necessary for formation of elastically effective PEO bridges), simply due to proximity. For amorphous PLA cores with fast dynamics, the chains rearrange to reach an equilibrium fraction of bridging chains in the gel. However, we hypothesize that the crystalline nature of the micelle cores in the 100/0 system, which forces chains to pack tightly and slows down their dynamics, may prevent some of the PEO chains from forming bridges. Although no PLLA

crystallites are detectable through WAXS in the samples that display the largest G' (75/25, 80/20, and 85/15), even if a small degree of crystalline order is present, this would significantly slow down the pull-out dynamics and influence the rheology. Thus, we hypothesize that micellar cores with a small amount of D-lactide are semicrystalline, comprising both amorphous regions and regions of either small or weakly ordered PLLA crystals. This structure would give chains enough mobility that they can more easily form bridges between micelles, promoting a larger fraction of bridging chains; while also leading to a long pull-out time for PLA endblocks.

Conclusions

We have demonstrated that associative hydrogels of PLA-PEO-PLA triblocks display novel rheology when the stereochemistry of the PLA block is varied. We find the unexpected result that there is a maximum in the storage modulus, G' , of the hydrogels at intermediate block lengths. This effect is quite dramatic; gels with PLA blocks with an L/D ratio of 85/15 have storage moduli that are ~1-2 orders of magnitude higher than the corresponding hydrogels formed from stereoregular systems. SANS results show a decrease in the intermicellar spacing for intermediate L/D ratios. Diffraction studies do not indicate formation of stereocomplexes in the gels, but do show PLLA crystals for gels with higher L-lactide content. We surmise that the rheology is due to a competition between an increase in the associative strength as PLLA crystals form and a decrease in the fraction of bridging chains, which may be disfavoured as the PLA cores become more crowded. Rheology at higher temperatures, as well as differential scanning calorimetry (DSC) experiments, may yield additional insight into whether PLLA crystallites that are too small to detect via WAXS are indeed present in micelles with intermediate L/D ratios. Additionally, nonlinear rheology measurements, in particular experiments that probe the recovery of these materials after large deformations and the behaviour under large-amplitude oscillatory shear, may provide information into the dynamics of endblock pull-out and network formation, which would aid in interpreting the physics of these types of networks. These results provide a new strategy for tuning the rheology of these and similar types of associative polymer systems, broadening their potential applications.

Conflicts of interest

There are no conflicts to declare.

Acknowledgements

The authors gratefully acknowledge financial support from NSF award CBET-1335787, ACS PRF grant 55729-ND9, Turner Dissertation Fellowship for D.R.O.H, and a Department of Education GAANN Fellowship (Award P200A160163) for S.P.Q. SANS experiments were conducted at the SNS, a DOE Office of Science User Facility operated by the ORNL. WAXS

experiments used beamline 11-BM of the NSLS II, a U.S. DOE Office of Science User Facility operated for the DOE Office of Science by BNL under Contract No. DE-SC0012704. The authors acknowledge assistance from Dr. Christopher Stanley, Dr. Michael Agamalian, and Dr. Luke Heroux at ORNL and Dr. Kevin Yager and Dr. Ruipeng Li at BNL. The sponsors had no role in the study design; in the collection, analysis and interpretation of data; in the writing of the report; and in the decision to submit the article for publication. The authors declare no competing financial interest.

References

- G. N. Tew, N. Sanabria-DeLong, S. K. Agrawal and S. R. Bhatia, *Soft Matter*, 2005, **1**, 253-258.
- S. K. Agrawal, N. Sanabria-DeLong, J. M. Coburn, G. N. Tew and S. R. Bhatia, *Journal of Controlled Release*, 2006, **112**, 64-71.
- S. K. Agrawal, N. Sanabria-DeLong, P. R. Jemian, G. N. Tew and S. R. Bhatia, *Langmuir*, 2007, **23**, 5039-5044.
- N. Sanabria-DeLong, S. K. Agrawal, S. R. Bhatia and G. N. Tew, *Macromolecules*, 2006, **39**, 1308-1310.
- A. T. Metters, K. S. Anseth and C. N. Bowman, *Journal of Physical Chemistry B*, 2001, **105**, 8069-8076.
- K. S. Anseth, A. T. Metters, S. J. Bryant, P. J. Martens, J. H. Elisseeff and C. N. Bowman, *Journal of Controlled Release*, 2002, **78**, 199-209.
- X. Garric, H. Garreau, M. Vert and J. P. Moles, *Journal of Materials Science-Materials in Medicine*, 2008, **19**, 1645-1651.
- I. Molina, S. M. Li, M. B. Martinez and M. Vert, *Biomaterials*, 2001, **22**, 363-369.
- H. T. Lee and D. S. Lee, *Macromolecular Research*, 2002, **10**, 359-364.
- S. M. Li, I. Rashkov, J. L. Espartero, N. Manolova and M. Vert, *Macromolecules*, 1996, **29**, 57-62.
- Z. B. Li, B. H. Tan, T. T. Lin and C. B. He, *Prog Polym Sci*, 2016, **62**, 22-72.
- D. K. Schneiderman and M. A. Hillmyer, *Macromolecules*, 2017, **50**, 3733-3750.
- L. Chen, Z. G. Xie, J. L. Hu, X. S. Chen and X. B. Jing, *J Nanopart Res*, 2007, **9**, 777-785.
- F. Nederberg, E. Appel, J. P. K. Tan, S. H. Kim, K. Fukushima, J. Sly, R. D. Miller, R. M. Waymouth, Y. Y. Yang and J. L. Hedrick, *Biomacromolecules*, 2009, **10**, 1460-1468.
- C. Hiemstra, Z. Y. Zhong, X. Jiang, W. E. Hennink, P. J. Dijkstra and J. Feijen, *J Control Release*, 2006, **116**, E17-E19.
- Y. I. Hsu, K. Masutani, T. Yamaoka and Y. Kimura, *Macromol Chem Phys*, 2015, **216**, 837-846.
- F. Li, S. M. Li and M. Vert, *Macromol Biosci*, 2005, **5**, 1125-1131.
- D. W. Lim, S. H. Choi and T. G. Park, *Macromol Rapid Comm*, 2000, **21**, 464-471.
- Y. Jing, C. Quan, B. Liu, Q. Jiang and C. Zhang, *Polymer Reviews*, 2016, **56**, 262-286.
- T. Fujiwara, T. Mukose, T. Yamaoka, H. Yamane, S. Sakurai and Y. Kimura, *Macromolecular Bioscience*, 2001, **1**, 204-208.
- R. M. Weiss, A. L. Short and T. Y. Meyer, *ACS Macro Lett*, 2015, **4**, 1039-1043.
- R. M. Weiss, J. Li, H. H. Liu, M. A. Washington, J. A. Giesen, S. M. Grayson and T. Y. Meyer, *Macromolecules*, 2017, **50**, 550-560.
- M. A. Washington, D. J. Swiner, K. R. Bell, M. V. Fedorchak, S. R. Little and T. Y. Meyer, *Biomaterials*, 2017, **117**, 66-76.
- S. K. Agrawal, N. Sanabria-DeLong, G. N. Tew and S. R. Bhatia, *Journal of Materials Research*, 2006, **21**, 2118-2125.
- S. Li, I. Rashkov, J. Espartero, N. Manolova and M. Vert, *Macromolecules*, 1996, **29**, 57-62.
- S. K. Agrawal, N. Sanabria-DeLong, G. N. Tew and S. R. Bhatia, *Macromolecules*, 2008, **41**, 1774-1784.
- K. A. Aamer, H. Sardinha, S. R. Bhatia and G. N. Tew, *Biomaterials*, 2004, **25**, 1087-1093.
- R. Agarwal, M. S. Alam and B. Gupta, *J Biomater Tiss Eng*, 2013, **3**, 273-283.
- D. G. Abebe and T. Fujiwara, *Biomacromolecules*, 2012, **13**, 1828-1836.
- H. A. Brown, A. G. De Crisci, J. L. Hedrick and R. M. Waymouth, *ACS Macro Lett*, 2012, **1**, 1113-1115.
- A. P. Dove, *ACS Macro Lett*, 2012, **1**, 1409-1412.
- B. G. Lohmeijer, R. C. Pratt, F. Leibfarth, J. W. Logan, D. A. Long, A. P. Dove, F. Nederberg, J. Choi, C. Wade and R. M. Waymouth, *Macromolecules*, 2006, **39**, 8574-8583.
- O. Coulembier, S. Moins, J.-M. Raquez, F. Meyer, L. Mespouille, E. Duquesne and P. Dubois, *Polymer degradation and stability*, 2011, **96**, 739-744.
- T. Isono, Y. Kondo, I. Otsuka, Y. Nishiyama, R. Borsali, T. Kakuchi and T. Satoh, *Macromolecules*, 2013, **46**, 8509-8518.
- D. Bigg, *Advances in Polymer Technology: Journal of the Polymer Processing Institute*, 2005, **24**, 69-82.
- M. A. V. Axelos and M. Kolb, *Phys Rev Lett*, 1990, **64**, 1457-1460.
- T. Matsumoto, M. Kawai and T. Masuda, *Macromolecules*, 1992, **25**, 5430-5433.
- J. M. Yu, P. Dubois, P. Teyssie, R. Jerome, S. Blacher, F. Brouers and G. LHomme, *Macromolecules*, 1996, **29**, 5384-5391.
- H. W. Richtering, K. D. Gagnon, R. W. Lenz, R. C. Fuller and H. H. Winter, *Macromolecules*, 1992, **25**, 2429-2433.
- C. R. Lopez-Barron, R. Chen, N. J. Wagner and P. J. Beltramo, *Macromolecules*, 2016, **49**, 5179-5189.
- K. Nagy-Smith, P. J. Beltramo, E. Moore, R. Tycko, E. M. Furst and J. P. Schneider, *ACS central science*, 2017, **3**, 586-597.
- H. H. Winter and F. Chambon, *Journal of rheology*, 1986, **30**, 367-382.
- D. Shin, K. Shin, K. A. Aamer, G. N. Tew, T. P. Russell, J. H. Lee and J. Y. Jho, *Macromolecules*, 2005, **38**, 104-109.
- Y. Takahashi and H. Tadokoro, *Macromolecules*, 1973, **6**, 672-675.
- J.-R. Sarasua, R. E. Prud'Homme, M. Wisniewski, A. Le Borgne and N. Spassky, *Macromolecules*, 1998, **31**, 3895-3905.
- G. Kokturk, E. Piskin, T. Serhatkulu and M. Cakmak, *Polymer Engineering & Science*, 2002, **42**, 1619-1628.
- A. N. Semenov, J. F. Joanny and A. R. Khokhlov, *Macromolecules*, 1995, **28**, 1066-1075.

ARTICLE

Journal Name

48. F. Tanaka and S. Edwards, *Macromolecules*, 1992, **25**, 1516-1523.
49. F. Tanaka and M. Ishida, *Macromolecules*, 1996, **29**, 7571-7580.
50. T. Annable, R. Buscall, R. Ettelaie and D. Whittlestone, *Journal of Rheology*, 1993, **37**, 695-726.
51. A. Semenov, J.-F. Joanny and A. Khokhlov, *Macromolecules*, 1995, **28**, 1066-1075.
52. M. Nguyen-Misra, S. Misra and W. L. Mattice, *Macromolecules*, 1996, **29**, 1407-1415.

Table of Contents Figure

Hydrogels of PLA-PEO-PLA display a striking enhancement of the stiffness at intermediate L/D ratio, demonstrating the impact of block stereochemistry on the rheology.

